bmo-miR-2739 and the novel microRNA miR-167 coordinately regulate the expression of the vitellogenin receptor in *Bombyx mori* oogenesis

Enxiang Chen[1,2], Zhiwei Chen[1,2], Shenglong Li[1,2], Dongxu Xing[3], Huizhen Guo[1,2], Jianqiu Liu[1,2], Xiaocun Ji[4], Ying Lin[1,2], Shiping Liu[1,2] and Qingyou Xia[1,2,*]

ABSTRACT

Vitellogenin receptors (VgRs) play crucial roles in oogenesis by mediating endocytosis of vitellogenin and other nutrients in ovipara. We conducted small RNA sequencing and screening with a luciferase reporter system, and found that bmo-miR-2739 and a novel miRNA (novel-miR-167) coordinately regulate the expression of *VgR* in *Bombyx mori* (*BmVgR*). Further analyses suggested that these two miRNAs direct target repression by binding directly to the *BmVgR* 3′ untranslated region. Forced expression of either miRNA using the *piggyBac* system blocked vitellogenin (Vg) transport and retarded ovariole development. Antagomir silencing of bmo-miR-2739 or novel-miR-167 resulted in increased amounts of BmVgR protein in the ovaries and *BmVgR* mRNA in the fat body. This evidence, combined with spatiotemporal expression profiles, revealed that these two miRNAs function together to fine-tune the amount of BmVgR protein for ovarian development. Additionally, novel-miR-167 was mainly responsible for the post-transcriptional repression of *BmVgR* in non-ovarian tissues. The results of this study contribute to our understanding of the function of miRNAs during ovarian development of a lepidopteran and suggest a new strategy for controlling insect reproduction.

KEY WORDS: MicroRNA, Transgene, Oogenesis, Vitellogenin receptor, *Bombyx mori*

INTRODUCTION

An inherently high reproductive capacity (rate) is an important strategy of insects, which enhances their chances of survival in nature and their ability to adapt to diverse ecological niches. However, excessive population growth causes many serious agricultural problems. Reproduction is tightly regulated via the process of oogenesis (Roy et al., 2018), which can be divided into three periods: previtellogenesis, vitellogenesis and choriogenesis (Funaguma et al., 2007; Yamauchi and Yoshitake, 1984). In vitellogenesis, vitellogenin (Vg) and a portion of the yolk proteins are transported from the haemolymph to the developing oocytes, ensuring the maturation of oocytes and the development of embryos (Roy et al., 2018; Yamauchi and Yoshitake, 1984). Vitellogenin receptors (VgRs) are crucial elements in the yolk protein transport process during this stage (Sappington and Raikhel, 1998). Because of the highly conserved modular structure of VgR in insects, its function is a subject of considerable research interest. Nevertheless, regulation of *VgR* gene expression has not been well studied, and the transcriptional regulation of *VgR* has only been reported in *Drosophila melanogaster* (Schonbaum et al., 2000), *Aedes aegypti* (Cho et al., 2006) and *Solenopsis invicta* (Chen et al., 2004). Research findings on the post-transcriptional and translational regulation of *VgR* in insects and other oviparous animals have not yet been published.

MicroRNAs (miRNAs) are small non-coding RNAs that drive post-transcriptional repression of mRNA targets in diverse eukaryotic lineages, and play key roles in many biological processes (Bartel, 2018; Lucas et al., 2015b), including female reproduction (Roy et al., 2018). Although the roles of miRNAs in reproductive events in the model organism, *D. melanogaster*, have been studied extensively (Garaulet et al., 2014; Ge et al., 2015; Huang et al., 2013; Nakahara et al., 2005; Roy et al., 2018; Stark et al., 2003), understanding miRNA function in non-*Drosophila* insect species is important for understanding the evolutionary variation of miRNA. Recently, functional studies of specific miRNAs in reproductive events have been reported in *A. aegypti* (Bryant et al., 2010; Lucas et al., 2015a; Liu et al., 2014; Zhang et al., 2016) and *Locusta migratoria* (He et al., 2016). The study of how miRNAs regulate the expression of the conserved VgR in insects is crucial for developing a full understanding of the regulatory processes of female insect reproduction and may suggest novel strategies toward the utilization of these small molecules for controlling insect propagation.

The domesticated silkworm *Bombyx mori* is a well-studied model in arthropod biology (Goldsmith et al., 2005; Izumi et al., 2016; Kiuchi et al., 2014; Tamura et al., 2000; Xia et al., 2014, 2009, 2004); it is also of interest owing to its huge economic impact in countries such as China and India. Its ovarian system makes it possible to isolate follicles in various developmental stages simultaneously from a single animal, which provides an excellent model for female reproductive and gene regulatory studies (Swevers and Iatrou, 2003). We carried out deep sequencing of small RNAs corresponding to vitellogenic and choriogenic follicles. By comparing the expression patterns of miRNAs in the two libraries along with a series of experimental verification studies, we found two miRNAs, bmo-miR-2739 and novel-miR-167, that affect the accumulation of Vg in follicles by regulating the temporal and spatial expression of VgR.

[1]Biological Science Research Center, Southwest University, Chongqing 400716, People's Republic of China. [2]Chongqing Key Laboratory of Sericulture Science, Southwest University, Chongqing 400716, People's Republic of China. [3]Sericulture and Agri-Food Research Institute, Guangdong Academy of Agricultural Sciences, Guangzhou 510610, China. [4]Research Center of Bioenergy & Bioremediation, College of Resources and Environment, Southwest University, Chongqing 400716, China.

*Author for correspondence (xiaqy@swu.edu.cn)

E.C., 0000-0002-0283-2463; Z.C., 0000-0001-8878-8784; S.L., 0000-0002-7841-572X; D.X., 0000-0002-1612-8661; H.G., 0000-0001-6895-9953; J.L., 0000-0003-0391-955X; X.J., 0000-0002-9981-0227; Y.L., 0000-0001-7452-4606; S.L., 0000-0002-2917-0172; Q.X., 0000-0002-9263-2886

RESULTS

Identification of two miRNAs targeted to BmVgR by small RNA sequencing analysis and luciferase reporter assay

To explore whether miRNAs are involved in regulating the expression of BmVgR, we divided an ovariole into five stages (V1, V2, C1, C2, C3) at pupal day 7 (P7D), and then conducted deep sequencing of two small RNA libraries derived from P7D follicles in vitellogenesis (V1) and choriogenesis (C3) (Fig. 1A'). We identified 257 novel miRNA candidates and 383 conserved miRNAs (Table S3). In examining the size distribution of total reads, we found a distinct bimodal distribution with a peak representing miRNAs 20-22 nucleotide (nt) long, and an increase in the total miRNA count from V1 to C3 (Fig. 1B). We found 242 different miRNAs between V1 and C3 (Table S4). We detected another distinct peak in the vicinity of 28 nt that mostly represented longer piwi-interacting RNAs (piRNAs), for which the total count dropped from V1 to C3 (Fig. 1B). Because both miRNA and piRNA act primarily as negative regulators, we hypothesized that the increased miRNAs from vitellogenesis to choriogenesis might contribute to the downregulation of physiological processes specific to vitellogenesis, such as VgR-mediated yolk protein uptake. Coincidentally, both BmVgR mRNA and protein were reduced from vitellogenesis to choriogenesis (Fig. 1A).

Typically, animal miRNAs bind seed match sites within the 3′ untranslated region (3′ UTR) of mRNAs (Zhang and Su, 2009). Using the target prediction program miRanda, we predicted the binding of 112 miRNAs to BmVgR 3′ UTR (thresholds were set to a score of 118 and less than −10 kcal/mol) (Table S5). There were 27 common miRNAs between the 112 predicted miRNAs of the BmVgR 3′ UTR and 242 differentially expressed miRNAs between V1 and C3 (Fig. 1C). The RNA-seq study contained only one developmental stage each at vitellogenesis and choriogenesis, which may not reflect the detailed expression pattern of these miRNAs, so we rechecked the expression pattern of these miRNAs
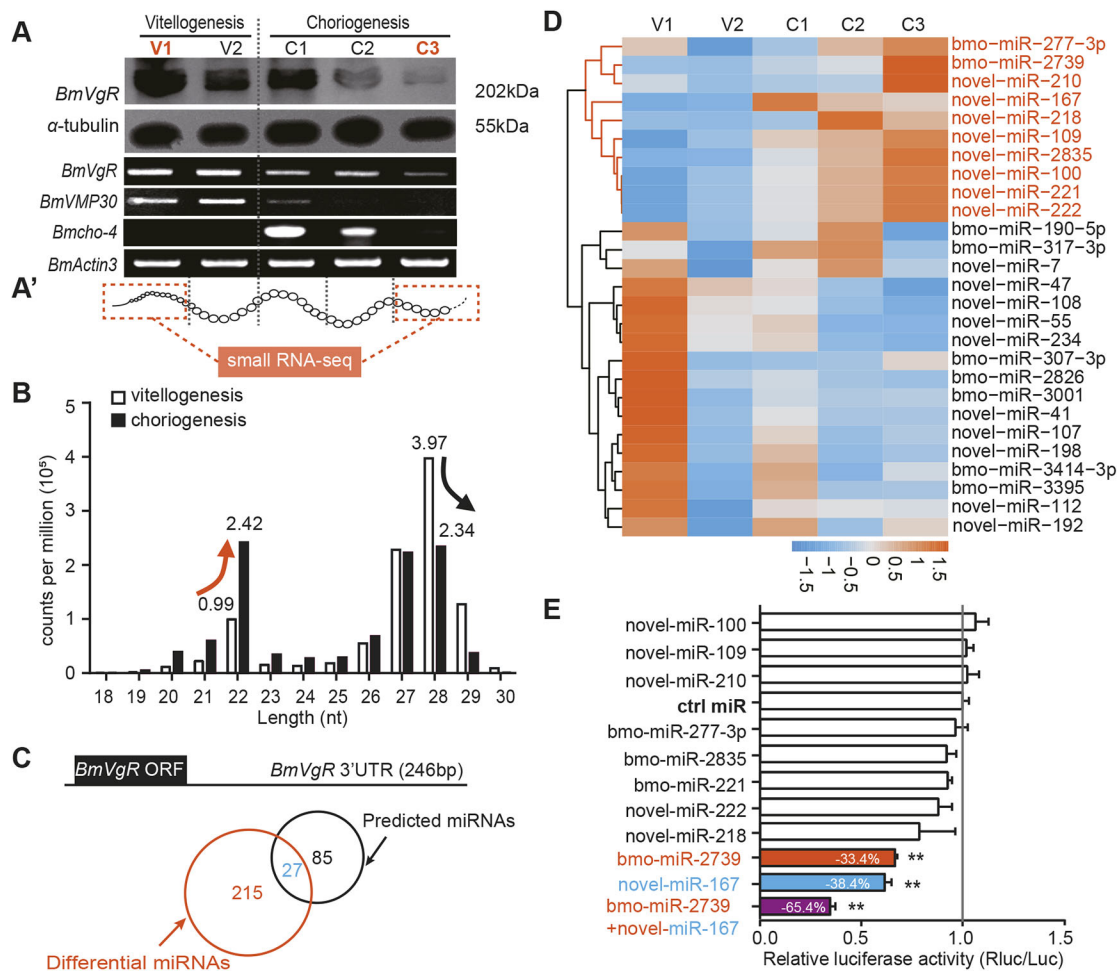

Fig. 1. Screening miRNAs that target BmVgR 3′ UTR. (A) Analysis of the expression patterns of BmVgR by western blot and RT-PCR. Criteria for partitioning one ovariole into five different stages were based on the marker genes Bmcho-4, a chorion gene expressed in early choriogenesis (Chen et al., 2015), and BmVMP30, which is mostly expressed in late vitellogenesis (Kendirgi et al., 2002). Housekeeping genes BmActin3 and α-tubulin were used as controls. (A′) Vitellogenesis contains stages V1 and V2, and choriogenesis contains stages C1, C2 and C3. Stages V1 and C3 (dashed boxes) were used for small RNA-seq. (B) Count distribution of small RNAs from 18 nt to 30 nt in vitellogenesis and choriogenesis libraries. The total number of molecules 22 nt long was 0.99×10^5 and 2.42×10^5 in vitellogenesis and choriogenesis libraries, respectively. The number of molecules 28 nt long was 3.97×10^5 and 2.34×10^5 in the two libraries. (C) Common miRNAs between miRNAs predicted within the BmVgR 3′ UTR (black ring) and miRNAs differentially expressed in the two small RNA libraries (brown ring). (D) qRT-PCR detection of the 27 common miRNAs from vitellogenesis to choriogenesis at P7D. (E) Screening miRNAs by a dual luciferase reporter (DLR) assay. Data are normalized to the median activity of the control miRNA mimic (ctrl miR). The activity was reduced 33.4%, 38.4% and 67.6% by bmo-miR-2739, novel-miR-167 mimic and both, respectively. These data represent three biological replicates with three technical replicates and error bars indicate s.e.m. ranges ($n=3$). **$P<0.01$ versus control (Student's t-test).

at intermediate stages in vitellogenesis and choriogenesis by qRT-PCR. Results suggested that 13 miRNAs increased from vitellogenesis to choriogenesis (Fig. 1E), most of which were consistent with the sequencing results (Table S3). Further, to assess the binding of these 13 miRNAs to the *BmVgR* 3′ UTR and to test whether these miRNAs regulated the expression of BmVgR, a psi-*BmVgR* 3′ UTR luciferase reporter plasmid and miRNA mimics were transfected into a human embryonic kidney 293T (HEK293T) cell line, followed by detection of luciferase activity 24 h later. Two miRNAs, bmo-miR-2739 and novel-miR-167, reduced the luciferase activity by 33.4% and 38.4%, respectively, compared with the negative control mimic, and the luciferase activity decreased 65.4% when both miRNAs were present (Fig. 1E).

Spatiotemporal expression analyses of BmVgR, bmo-miR-2739 and novel-miR-167

Comparing the expression of bmo-miR-2739 and novel-miR-167 with that of BmVgR could provide clues to the regulatory effects of the two miRNAs. In 2013, Lin et al. reported that the expression of *BmVgR* mRNA was high in ovarian tissue at prepupal and pupal stages using reverse transcription PCR (RT-PCR) (Lin et al., 2013). Therefore, we conducted expression analyses at different ovarian stages during day 5 of the 5th larval instar (L5D5), days 1-3 of wandering and pupal days 3-4 based on qRT-PCR to monitor RNA accumulation and western blot for BmVgR protein. *BmVgR* mRNA increased from day 2 of wandering (W2D) to maximum expression at W3D. BmVgR protein maintained a higher expression at P3D and P4D (Fig. 2A), whereas bmo-miR-2739 and novel-miR-167 exhibited lower expression at these stages than at larval stages (Fig. 2B).

To determine the change in expression of these two miRNAs during the transition from vitellogenesis to choriogenesis, we extracted total RNA from single eggs and used vitellogenic and choriogenic marker genes (*BmVMP30* and *Bmcho-4*) to identify the transitional egg. qRT-PCR results indicated that the expression of

these two miRNAs started to increase from the transition point between the two developmental stages (Fig. 2C). In pooled developing eggs, the expression of novel-miR-167 reached its maximum at C1, which was earlier than bmo-miR-2739 (at C3) (Fig. 1D). The expression of BmVgR protein decreased after C2 and reached its lowest level by C3 (Fig. 1A). These results indicated that the expression of bmo-miR-2739 increased continuously from the transition point to late choriogenesis, whereas novel-miR-167 only had a peak near the transition point.

Among the different tissues assayed, the mRNA and protein levels of BmVgR were most highly expressed in ovarian tissue (Fig. 2D). BmVgR protein was not detected in other tissues, such as fat body and silk gland, although a small amount of *BmVgR* mRNA was present (Fig. 2D). Further, bmo-miR-2739 exhibited higher expression in ovary than in some other tissues, whereas novel-miR-167 exhibited much lower expression in the ovary than in other tissues (Fig. 2E, Fig. S1C). The expression profiles of these two miRNAs indicated that their concentrations were inversely correlated to the amounts of BmVgR protein at different developmental stages of ovary, which reflected a possible regulatory relationship between them.

A BLASTn search in NCBI with the pre-bmo-miR-2739 sequence revealed highly similar sequences in other Lepidoptera, such as *Calycopis cecrops*, *Papilio machaon*, *Melitaea cinxia* and *Spodoptera litura*; however, the pre-novel-miR-167 was found only in *B. mori* (Fig. S1A,B). This indicated bmo-miR-2739 may have a homologue in other insect species, whereas novel-miR-167 may be functionally specific to silkworms.

bmo-miR-2739 and novel-miR-167 reduced the expression of BmVgR by binding to the *BmVgR* 3′ UTR directly

miRNA target prediction suggested three possible binding sites for bmo-miR-2739 in the *BmVgR* 3′ UTR (+182, +77 and +53) and only one (+109) for novel-miR-167 (Fig. 3A, Fig. S2A,B). A dual-luciferase reporter assay system (DLR) was used to check whether
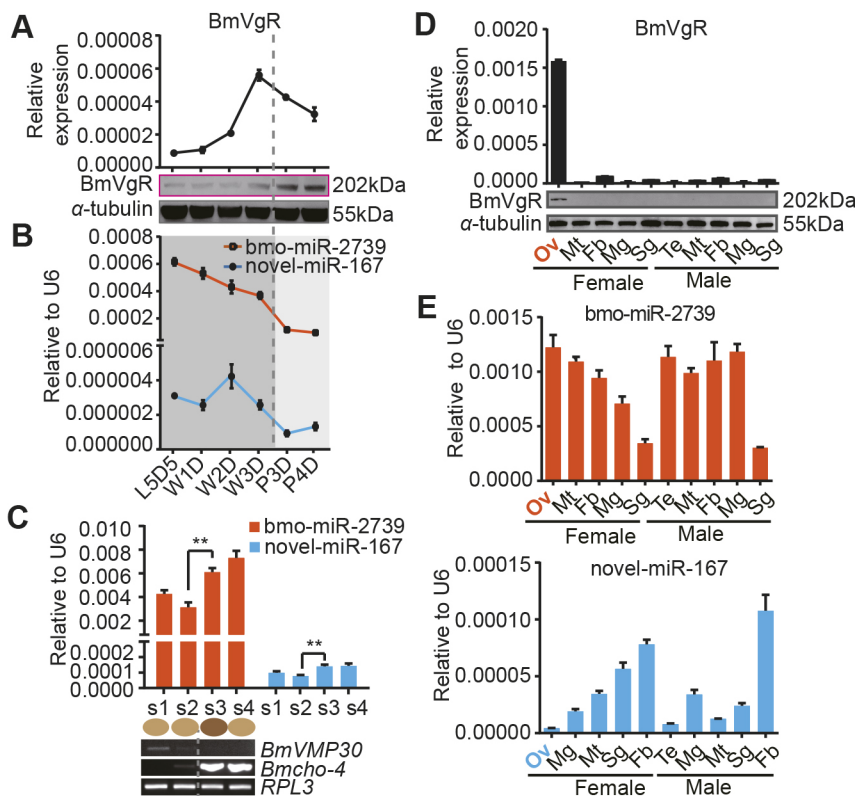

Fig. 2. Spatiotemporal expression analyses of BmVgR, bmo-miR-2739 and novel-miR-167.
(A,B) Expression analysis of BmVgR, bmo-miR-2739 and novel-miR-167 in different ovarian stages by western blot and qRT-PCR. (C) Analysis of the expression of the two miRNAs in single eggs at the transition point from vitellogenesis to choriogenesis at P7D. Top: Expression of the two miRNAs near the transition point determined by qRT-PCR. s1-s4 indicate different follicular stages. Bottom: *Bmcho-4* and *BmVMP30* used to distinguish the transition between vitellogenesis and choriogenesis by RT-PCR. (D,E) Analyses of the expression of BmVgR, novel-miR-167 and bmo-miR-2739 in different tissues at W2D by western blot and qRT-PCR. Mean values and s.e.m. for three replicates are shown. Fb, fat body; Mg, midgut; Mt, Malpighian tubule; Ov, ovary; Sg, silk gland; Te, testis. All data represent three biological replicates with three technical replicates, error bars indicate s.e.m. ranges (*n*=3). **P<0.01 (Student's *t*-test).
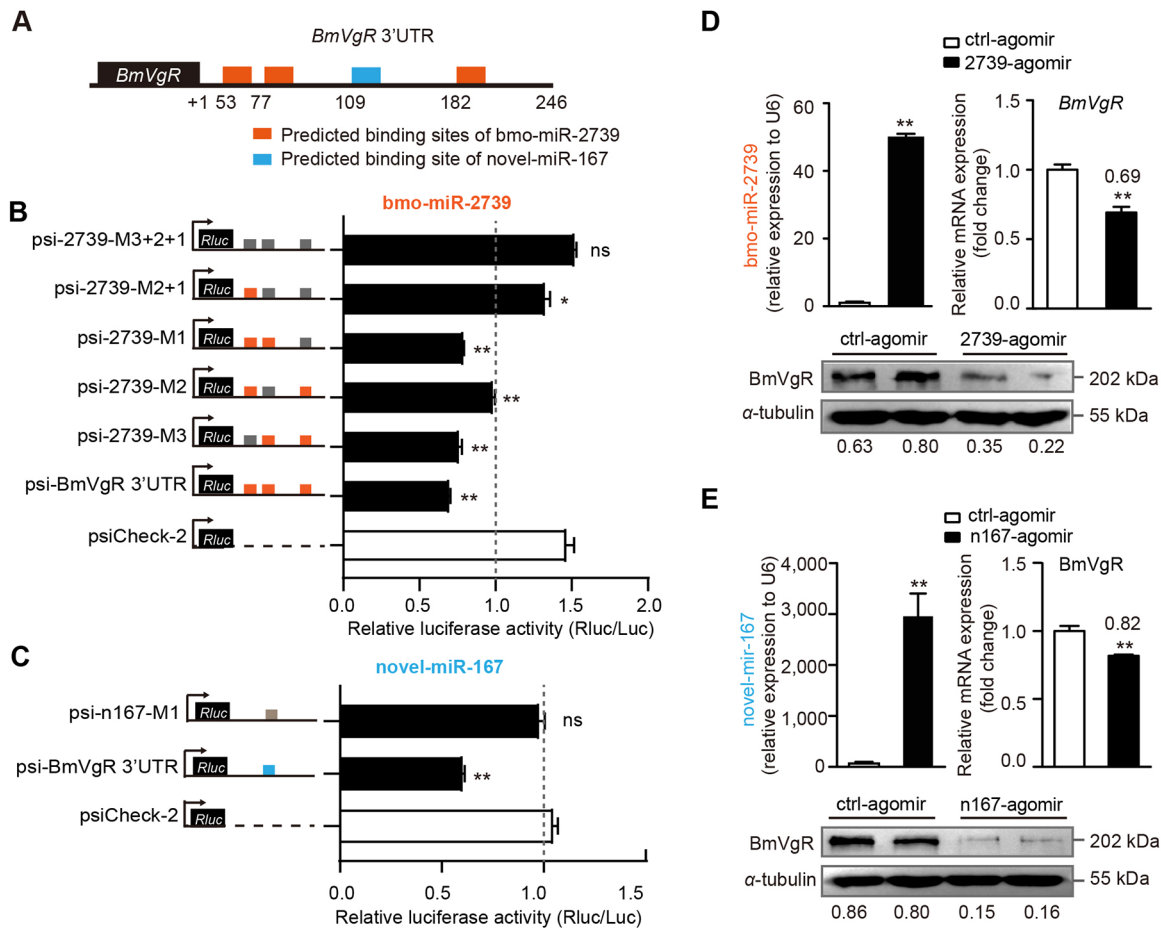
Fig. 3. The gene encoding the BmVgR is the direct target of bmo-miR-2739 and novel-miR-167. (A) Predicted binding sites of bmo-miR-2739 (orange blocks: +182, +77 and +53) and novel-miR-167 (blue block: +109) in *BmVgR* 3′ UTR. (B,C) Effects of the two miRNAs on the activities of the luciferase reporter constructs with the full-length and different mutated *BmVgR* 3′ UTRs. HEK293T cells were transfected with different constructs for 6 h, followed by transfection with miRNA agomir (100 nM) or ctrl-agomir (100 nM) for 24 h. The effect of ctrl-agomir on the luciferase activities of different constructs was defined as 1.0. Small grey blocks represent mutations at the binding sites. (D,E) Overexpression of novel-miR-167 and bmo-miR-2739 using miRNA agomir (200 nM) downregulated mRNA and protein levels of BmVgR in BmN4-SID1 cells. Data were normalized to the median of the control group. Numbers in the lower panel indicate the relative density of BmVgR protein compared with α-tubulin. *$P<0.05$, **$P<0.01$ (two-tailed Student's *t*-tests). Error bars indicate s.e.m. ranges ($n=3$). ns, not significant.

these two miRNAs could directly bind to the predicted 'seed'-binding sites of the *BmVgR* 3′ UTR using six reporter vectors constructed with mutations in them (Fig. 3B,C). HEK293T cells and S2 cells were transfected with different reporter plasmids and miRNA agomirs, and luciferase activity was detected after 24 h. Luciferase activity was notably reduced compared with controls after transfection with a psi-BmVgR 3′ UTR reporter plasmid and either of the two agomirs. However, no reduction was observed with mutations in the predicted seed-binding sites of the *BmVgR* 3′ UTR, and the binding site in +77 was the most important for the binding of bmo-miR-2739 in both HEK293T cells and S2 cells (Fig. 3B,C, Fig. S2C,D). These findings indicated that bmo-miR-2739 and novel-miR-167 bound to the predicted binding sites within *BmVgR* 3′ UTR.

In addition, bmo-miR-2739 agomir (2739-agomir) or novel-miR-167 agomir (n167-agomir) was transfected into the ovarian cell line BmN4-SID1, which contains an endogenous BmVgR. bmo-miR-2739 reduced BmVgR mRNA and protein levels by 31% and at least 44% (Fig. 3D), respectively, and novel-miR-167 reduced those mRNA and protein levels by 18% and at least 80% (Fig. 3E). These results indicated that bmo-miR-2739 and novel-miR-167 could bind to the *BmVgR* 3′ UTR and mediate the post-transcriptional repression of *BmVgR* mRNA.

Establishment of transgenic silkworm lines expressing bmo-miR-2739 and novel-miR-167

To investigate further the role of bmo-miR-2739 and novel-miR-167 in the development of the ovary, we chose a polymerase III U6-promoter cloned from *B. mori* (Tanaka, 2013) to express the precursor of these two miRNAs (Fig. 4A). Two positive transgenic lines (U6-2739 and U6-n167) were obtained by visualizing fluorescent screening of 3xp3-EGFP expression in the eyes (Fig. S3A,B). Inverse PCR analyses suggested that the U6-2739 vector and U6-n167 vector were integrated into the fifth intron of gene BGIBMGA009981 and the first intron of gene BGIBMGA002981 (Fig. S3A′,B′) without affecting their expression (Fig. S3C). Comparison of transgenic and wild-type (WT) expression of bmo-miR-2739 and novel-miR-167 in ovarioles and the fat body at P6D indicated increases of 2.1-fold and 1.8-fold, respectively. Expression of bmo-miR-2739 and novel-miR-167 increased most in the male fat body, reaching 20.8-fold and 6.7-fold, respectively, compared with controls (Fig. S3D,E). These results suggested these two miRNAs were successfully expressed using the U6 promoter.

Additionally, we found increased expression of bmo-miR-2739 in the U6-n167 transgenic strain and novel-miR-167 in the U6-2739 transgenic strain. The expression facilitated by novel-miR-167
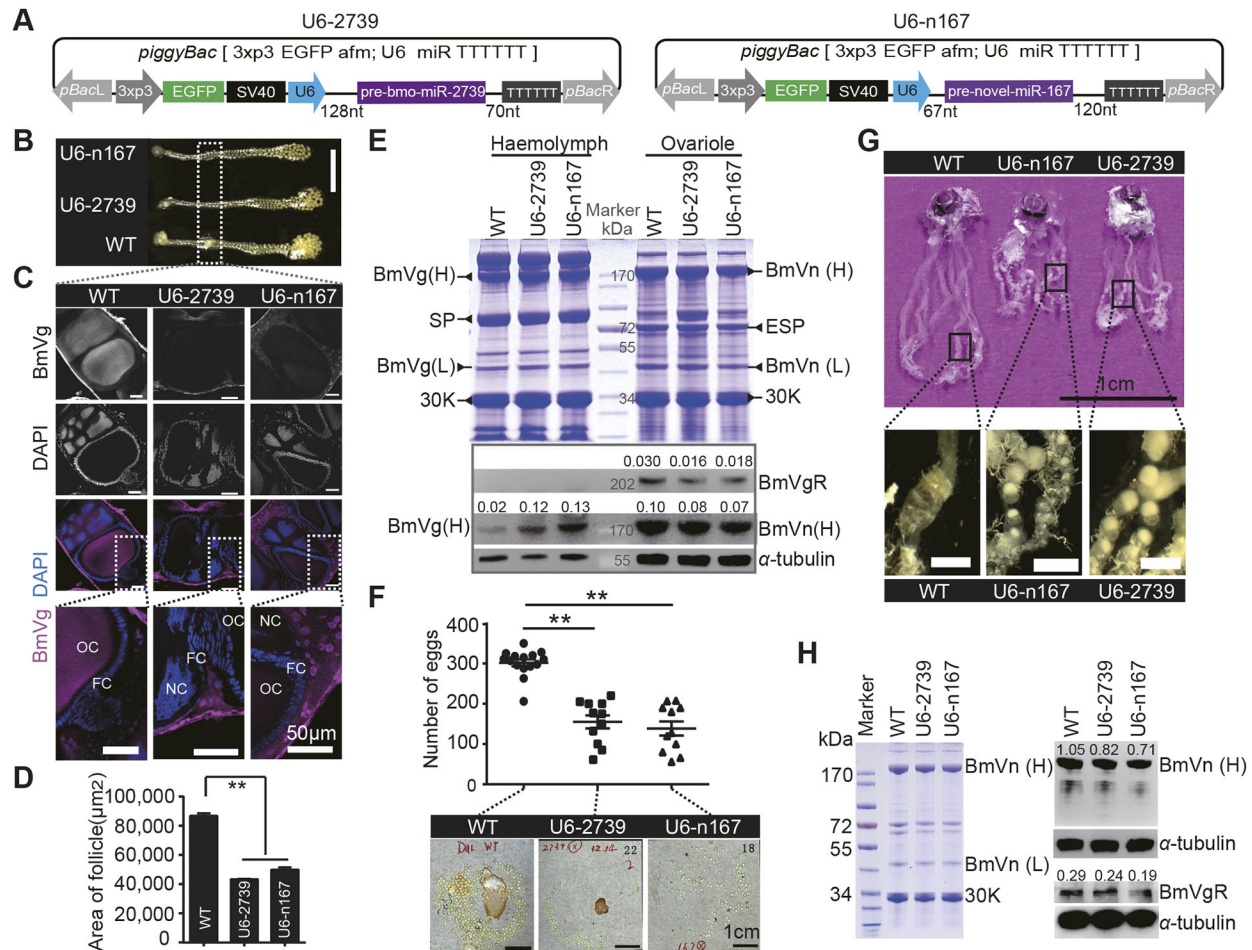
Fig. 4. Effects of overexpression of bmo-miR-2739 or novel-miR-167 on the development of eggs in transgenic silkworms. (A) Schematic of the transgenic vectors for pre-bmo-miR-2739 and pre-novel-miR-167. The two miRNAs were driven by a U6 promoter and ended with 'TTTTTT'. The transgenic screening cassette was constructed with an *EGFP* reporter gene driven by the 3xp3 promoter and be adjacent to SV40 poly (A) terminator (see Materials and Methods). (B) Ovarioles dissected from the transgenic silkworms (U6-2739 and U6-n167) and WT silkworms at P6D. Scale bar: 1 cm. The dashed box indicates the part that was used for immunofluorescence localization of BmVn protein. (C) Localization of BmVn in the follicle determined by immunofluorescence. FC, follicular epithelial cell; NC, nurse cell; OC, oocyte. (D) Follicle size for U6-2739, U6-n167 and WT. (E) Protein analysis of the transgenic silkworms. Top: Analysis of total proteins from the fat body, haemolymph, and ovaries of female moths by SDS-PAGE. Bottom: analysis of BmVg/BmVn protein by western blot analysis. Numbers represent relative density of proteins compared with α-tubulin. 30 K, 30-kDa proteins; ESP, egg-specific protein; H, heavy subunit; L, light subunit; SP, storage proteins. (F) Egg-laying number in U6-2739, U6-n167 and WT. (G) Ovarioles in laid eggs of U6-2739, U6-n167 and WT. The images in the lower panel were visualized with a Zeiss Stemi 2000-C stereo microscope. Scale bars: 0.5 cm (lower panels). (H) Analysis of total protein and BmVn/BmVgR protein in 20 laid eggs by SDS-PAGE and western blot analysis. Numbers represent relative density of proteins compared with α-tubulin. All data represent four biological replicates with three technical replicates and are shown as mean±s.e.m. (n=3); **P<0.01 versus WT (Student's *t*-test).

seemed even stronger than that induced by bmo-miR-2739 (Fig. S3G,H). These data suggested that there might be a mutually reinforcing mechanism between the two miRNAs.

Forced expression of bmo-miR-2739 or novel-miR-167 hampered the development of eggs in transgenic silkworms

We successfully ectopically overexpressed the miRNAs in the ovarioles of transgenic silkworms (Fig. S3D,E) and found that the development of the ovariole in the two transgenic strains was slower than in WT, with the U6-n167 strain being slowest (Fig. 4B). This indicated that only a 1.8-fold increase in the expression of novel-miR-167 in ovaries can delay egg development; furthermore, the degree of delay was greater than that produced by a 2.1-fold increase of bmo-miR-2739. To determine the physiological basis of the delayed egg development, we examined the distribution of yolk protein in the follicles. Transported vitellogenin (BmVg) from haemolymph to the follicle is stored in a crystalline form as vitellin

in *B. mori* (BmVn) (Lin et al., 2013). The immunofluorescence localization of BmVn showed that although it was widely distributed in WT oocytes and nurse cells, only a small amount accumulated in the oocytes of the two transgenic strains. Additionally, a large amount of BmVg protein was found on the periphery of transgenic follicles (Fig. 4C), which were notably smaller than those of the WT group at the same stage (Fig. 4D). SDS-PAGE analysis suggested that the main haemolymph proteins (BmVg, storage proteins, 30-kDa proteins) are expressed at P7D (Fig. 4E). Western blot results indicated an increase in BmVg haemolymph protein and a reduction in BmVn egg protein in the two transgenic strains. BmVgR protein decreased more in the two transgenic strains than in the control group (Fig. 4E). The egg-laying rate of the two transgenic strains was also significantly lower than that of the control group (Fig. 4F). Dissection of the moths after egg laying revealed numerous undeveloped follicles in the two transgenic strains and developmentally earlier eggs in the U6-n167

strain than in the U6-2739 strain (Fig. 4G). Analysis of protein content by SDS-PAGE indicated that BmVn and 30-kDa proteins (30 K) in mature eggs exhibited different degrees of decline in transgenic individuals (Fig. 4H). Western blot results indicated a reduction in BmVn egg protein in the U6-2739 and U6-n167 strains by 21.9% and 32.4%, respectively. BmVgR protein decreased more in transgenic individuals than in the controls, and decreased most in the U6-n167 strain (Fig. 4H). These observations indicated that forced expression of these two miRNAs resulted in reduction of BmVgR protein and retardation of ovariole development.

Because of the low expression of *BmVgR* mRNA and novel-miR-167 in testes of WT silkworms (Fig. 2D,E), we considered the expression of *BmVgR* mRNA in testes of the two transgenic strains. Despite increasing the expression of bmo-miR-2739 and novel-miR-167 by 2.2-fold and 2.1-fold, respectively, in testes, the expression of *BmVgR* mRNA, which was already weak, still decreased by 10.2% and 66.6% in U6-2739 and U6-167 transgenic strains, respectively (Fig. S3F). This suggested that novel-miR-167 exerted more powerful post-transcriptional repression in testes than bmo-miR-2739.

The results described above verified that the independent forced expression of bmo-miR-2739 or novel-miR-167 in transgenic silkworms significantly reduced the rate of egg-laying and development. Next, we wanted to understand what would happen if these two miRNAs were overexpressed in a single transgenic silkworm. To do so, we mated the genetically modified U6-2739 and U6-n167 individuals. Because these two transgenic strains were both screened using an EGFP reporter gene and could not be differentiated visually by fluorescence, we took the old cuticle shed from larvae to pupae of the first generation (G1) of hybridized transgenic silkworms for genomic extraction. Genomic PCR results (Fig. S4A,B) allowed us to identify 34 individuals (15 females and 19 males) that expressed these two miRNAs simultaneously in the G1 hybrids (named strain U6-2739+U6-n167). Hybrid female pupae were larger than the WT pupae, but there was no significant difference compared with the size of hybrid males (Fig. S4D). Furthermore, we discovered that some of the abnormally large hybrid female pupae had no obvious egg formation (Fig. S4E). qRT-PCR also indicated that a large amount of bmo-miR-2739 and novel-miR-167 had accumulated throughout their bodies (Fig. S4F). In some U6-2739+U6-n167 pupae, ovariole development was seriously blocked and the BmVgR protein and mRNA levels were low (Fig. S4G,H). Further, bmo-miR-2739 and novel-miR-167 increased by 4.8-fold and 51.0-fold more, respectively, in the follicles of the U6-2739+U6-n167 strain than in their respective single miRNA overexpression strain (Fig. S4I). These results suggested that the forced expression of both bmo-miR-2739 and novel-miR-167 led to increased retardation of egg development compared with expression of a single miRNA.

Inhibition of miRNAs increased the BmVgR protein output

We used bmo-miR-2739 and novel-miR-167 antagomirs (2739-anta and n167-anta) and inhibitors (2739-inh and n167-inh) to verify the effect of inhibition of endogenous miRNAs on the expression of BmVgR in silkworms and BmN4-SID1 cells. After injection of 2739-anta and n167-anta into experimental silkworm groups, the endogenous miRNAs in ovarioles decreased by 48.2% and 28.6%, respectively, at P8D (Fig. 5B,B′), and the BmVgR and BmVn protein output was greater in both antagomir-treated animals than in the control group (Fig. 5C′). However, *BmVgR* mRNA was decreased in experimental groups (Fig. 5C). Nonetheless, we did not observe a significant phenotypic change in ovariole development (Fig. 5A,A′). In the fat body, which had the highest non-ovarian tissue expression of
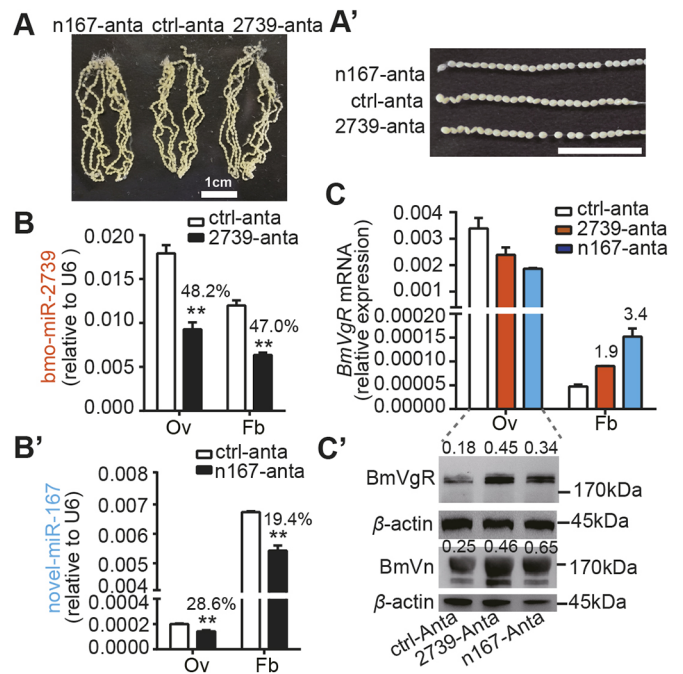

Fig. 5. Effects of 2739-anta and n167-anta injection on the expression of BmVgR. (A,A′) Ovarioles dissected from injected miRNA antagomir silkworms (2739-anta and n167-anta) and control antagomir silkworms (ctrl-anta) at P8D. Scale bars: 1 cm. (B,B′) Detection of the two miRNAs in ovarioles (Ov) and the fat body (Fb) at P8D by qRT-PCR analysis. (C,C′) Detection of *BmVgR* mRNA and BmVgR/BmVn protein in ovarioles at P8D. BmVgR/BmVn antibody and β-actin antibody were used as primary antibodies; numbers represent the relative density of BmVgR/BmVn protein compared with β-actin. All data represent three biological replicates with three technical replicates and are shown as an average±s.e.m. (*n*=3); **P<0.01 relative to ctrl-anta (Student's *t*-test).

BmVgR mRNA (Fig. 2D), the endogenous miRNAs decreased by 47.0% and 19.4% after exposure to 2739-anta and n167-anta, respectively (Fig. 5B,B′), which was accompanied by increased expression of *BmVgR* mRNA by 1.9-fold and 3.4-fold (Fig. 5C). Nevertheless, we failed to detect the expression of BmVgR protein in the fat body, probably because of the inhibitory effect of the miRNAs. On the other hand, the expression of endogenous bmo-miR-2739 and novel-miR-167 was reduced by 46.4% and 37.5% in BmN4-SID1 cells after transfection with bmo-miR-2739 inhibitor (2739-inh) and novel-miR-167 inhibitor (n167-inh), respectively, accompanied by increased expression of BmVgR at both the mRNA and protein levels as determined by qRT-PCR and western blot analysis (Fig. S5A,B). The addition of purified BmVg protein to BmN4-SID1 cells that had been transfected with 2739-inh and n167-inh resulted in an increased uptake of BmVg compared with the control (Fig. S5C,D). These results indicated that inhibition of endogenous miRNAs weakened post-transcriptional repression and led to increased BmVgR protein in the ovaries and the BmN4-SID1 cell line. Inhibition of endogenous miRNAs also affected the transport of the BmVg protein. In the fat body, the post-transcriptional repression of novel-miR-167 was greater than that of bmo-miR-2739. In the ovary, however, the repression of novel-miR-167 decreased owing to its low concentration.

DISCUSSION
VgR is an important receptor for ovarian development in ovipara (Sappington and Raikhel, 1998; Tufail and Takeda, 2009). To date, research on the 5′ regulatory region and specific transcription

factors that control transcription of the *VgR* mRNA has been limited to a few insects (Chen et al., 2004; Cho et al., 2006; Schonbaum et al., 2000) and fish (Dominguez et al., 2014), and the studies of post-transcriptional regulation are limited. We found that bmo-miR-2739 and novel-miR-167 separately regulated the expression of BmVgR by directly binding to the *BmVgR* 3′ UTR. To verify the regulatory roles of these two miRNAs, we overexpressed and inhibited the two miRNAs *in vitro* and *in vivo* and found that bmo-miR-2739 and novel-miR-167 could cooperatively direct the post-transcriptional repression of *BmVgR*.

When we forced these two miRNAs to overexpress in silkworm, we observed a developmental retardation of the eggs and a decrease of the egg-laying rate. In the two transgenic strains, the main haemolymph proteins (storage proteins, BmVg, 30 K), which are synthesized in the pupal fat body, did not decrease, but increased. In addition, there was less BmVn protein in eggs of the two transgenic strains than in WT (Fig. 4E), leading to fewer eggs produced (Fig. 4B) or none (Fig. S4E). These findings were similar to the phenotype recorded in the *vit/vit* silkworm mutant, which carries a deficient *BmVgR* gene (Kawaguchi et al., 2008; Lin et al., 2013), and in silkworms with RNAi silencing of *BmVgR* (Lin et al., 2013). Vg protein is secreted in the haemolymph and transported into the ovary by VgR-mediated endocytosis (Tufail and Takeda, 2009). If the synthesis of BmVg protein in the fat body were unaffected in the two transgenic strains, but the BmVgR protein was markedly reduced by the excess miRNAs, it should have resulted in BmVg accumulation in the haemolymph and ultimately led to reduced or no egg production. So far, we have observed no decrease in the main haemolymph proteins, which suggests that the two overexpressed miRNAs have little effect on the synthesis of proteins in the fat body, but we cannot rule out the effect of these two miRNAs on the synthesis of other small molecules. Nevertheless, our results at the cellular level strongly suggest a direct and unambiguous regulation effect of these two miRNAs on BmVgR. We believe that the reason for the reduced egg-laying rate is the decreased expression of BmVgR caused by these two miRNAs. These results indicate that forced expression of these two miRNAs in ovaries dampen the expression of BmVgR, block the transport of BmVg from haemolymph to oocyte, and result in retardation of ovariole development.

When we injected the two miRNA antagomirs, although we detected an induced expression of BmVgR and also observed an increase of BmVn in eggs, we did not observe any marked phenotypic changes in egg production. Our current results provide preliminary evidence of the regulatory relationship between the two miRNAs and BmVgR, as well as the enhancement of BmVg protein uptake into oocytes by miRNA inhibition. Upregulated BmVgR expression alone may not be sufficient to alter egg development if the nutrients synthesized by the fat body remain unchanged. In the future, it may be possible to increase insect fecundity if both an incremental expression of yolk proteins and an increased expression of VgR by changing the expression of regulatory factors like bmo-miR-2739 and novel-miR-167 can be achieved through genetic approaches.

It is important to understand whether these two miRNAs dampen translation initiation or degrade mRNA, or both. When we forced these two miRNAs to overexpress in ovarian cells, we observed only weak changes in the level of *BmVgR* mRNA, but there was a notable change in the level of BmVgR protein (Fig. 3D,E). Moreover, termination of *BmVgR* mRNA transcription (Zhang et al., 2017) and a decrease of BmVgR protein (Fig. 1A) are observed when the majority of follicles enter choriogenesis. However, in our study *BmVgR* mRNA was decreased, and BmVgR protein was induced in the two miRNAs inhibition groups at this stage (Fig. 5C,C′). We

propose that the higher amount of BmVgR protein than that of control group is due to the weakening of BmVgR translation inhibition caused by the two miRNAs, and that *BmVgR* mRNA consumption in the translation process leads to the decline of *BmVgR* in the two miRNA inhibition groups. This demonstrates that the two miRNAs mainly inhibited the post-transcriptional or translational level of *BmVgR*.

There are two possible reasons for the slight decrease of *BmVgR* mRNA in ovarian cells. One possibility is that the two miRNAs elicit translational repression, which also ultimately triggers mRNA degradation; this mechanism has been reported in *Drosophila* (Djuranovic et al., 2012) and zebrafish (Bazzini et al., 2012). Another possibility is that the two miRNAs affect the transcription of *BmVgR* by regulating other target genes. The detailed post-transcriptional repression mechanism of these two miRNAs and possible indirect effects on the transcriptional level need further study. In addition, there may be a mutually reinforcing mechanism between the two miRNAs, further enhancing the post-transcriptional repression of *BmVgR*. The specific regulatory mechanism between these two miRNAs also needs further exploration.

When we analysed the spatiotemporal expression patterns of these two miRNAs and BmVgR, we found that they may be involved in the stage-specific and tissue-specific expression of BmVgR. The inhibition function of miRNA is mainly determined in two different ways, via the complementarity of miRNA: mRNA interaction and the differential expression of miRNA (Bartel, 2009, 2018). bmo-miR-2739 and novel-miR-167 have three weak complementarity sites and extensive complementarity within the *BmVgR* 3′ UTR, respectively (Fig. S2A,B). Additionally, DLR assays showed that the inhibition of novel-miR-167 was stronger than that of bmo-miR-2739 (Fig. 1E, Fig. S2C,D). At different developmental stages of the ovary, novel-miR-167 appeared to respond more quickly to relieve its inhibiting effect compared with bmo-miR-2739, given that the concentration of novel-miR-167 was downregulated from an earlier stage (W2D) and had extensive complementarity within the *BmVgR* 3′ UTR. Moreover, the expression level of bmo-miR-2739 significantly decreased after W3D. After entering the pupal stage, both miRNAs exhibited relatively low expression levels, similar to the relatively low inhibition of the expression of BmVgR. Thus, regulation of BmVgR protein expression reached the optimal level in vitellogenic follicles and ensured their nutritional supply. Furthermore, at the beginning of follicle vitellogenesis, VgR protein mainly plays a transport function with high expression. By the end of vitellogenesis, the receptor begins to decline (Tufail and Takeda, 2009). Combined with the expression pattern of these two miRNAs from vitellogenesis to choriogenesis (Figs 1D, 2C), our results suggest that when the follicle enters choriogenesis, increased novel-miR-167 and bmo-miR-2739 bind to the complementary sites within the *BmVgR* 3′ UTR and exert a high level of inhibition of the expression of BmVgR protein. novel-miR-167 also seems to respond more quickly to perform inhibitory functions than does bmo-miR-2739. In this way, these two miRNAs act cooperatively to fine-tune the expression of BmVgR for different development stages of the ovary.

To prevent BmVgR protein from expressing in non-ovarian tissues, the cell can come to depend on its milieu of miRNAs to act as binary off-switches to help to repress BmVgR protein output to inconsequential levels. The effect of novel-miR-167 is more powerful than bmo-miR-2739 in the female fat body (Fig. 5C) and testes (Fig. S3F). This suggests that because of the high expression of novel-miR-167 in non-ovarian tissues and its extensive complementarity to *BmVgR* 3′ UTR, novel-miR-167 is adjusted to high inhibition in
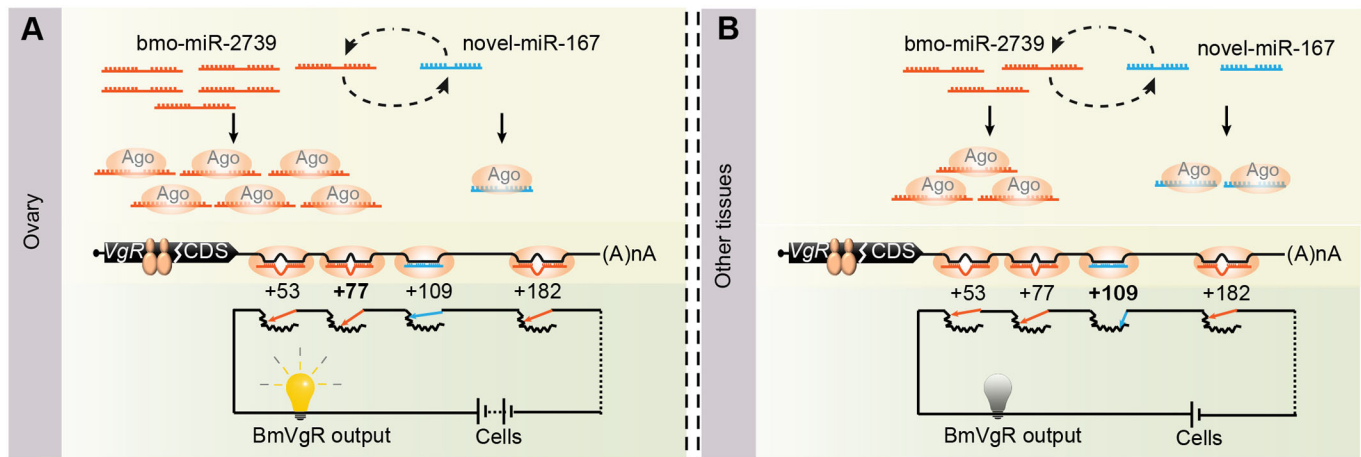
Fig. 6. Schematic summarizing the regulatory relationship between the two miRNAs and BmVgR. The combinatorial rheostat analogy of the miRNA: *BmVgR* mRNA interaction. Each miRNA complementary site within the *BmVgR* 3′ UTR is analogous to a rheostat (Rheostat +53, +77, +182 for bmo-miR-2739 and Rheostat +109 for novel-miR-167), the same as an adjustable resistor (zig-zag arcs indicate a resistor; orange and blue arrows indicate the adjustment). The brightness of the lamp bulb represents the amount of BmVgR protein produced. The cells represent the amount of *BmVgR* mRNA. (A) In the ovary, rheostat +109 is adjusted to low resistance because novel-miR-167 is expressed at low levels. In this case, it is the high level of the 'orange' bmo-miR-2739 expression in ovary that ensures that the complementary site is almost fully occupied despite its three weak complementarity sites to the 'orange' bmo-miR-2739. Rheostat +53, +77, +182 are adjusted to appropriate resistances, which ensures the optimal BmVgR protein level for ovary. These two miRNAs act cooperatively to fine-tune the 'resistance' changes of BmVgR expression for different development stages of the ovary. (B) In non-ovarian tissues, rheostat +109 is adjusted to high resistance based on its higher expression than in ovary and extensive complementarity to 'blue' novel-miR-167. novel-miR-167, ensuring that, together with bmo-miR-2739, and despite the low 'resistance' of bmo-miR-2739, the 'leaky' transcription of *BmVgR* mRNA will not produce protein.

non-ovarian tissues, together with bmo-miR-2739, despite the low inhibition of bmo-miR-2739, ensuring that the 'leaky' transcription of *BmVgR* mRNA will not produce protein. We conclude that in non-ovarian tissues novel-miR-167 mainly regulates the post-transcriptional repression of BmVgR.

The resistor analogy previously proposed by Bartel and Chen (2004) seems a fitting model for the post-transcriptional repression of the two miRNAs we report here (Fig. 6A,B). In this analogy, expression of a target gene that responds to the presence of miRNAs decreases just as an adjustable resistor in an electric circuit causes the current to decrease. The 'resistance' is adjusted in two different ways, via the complementarity of miRNA: by mRNA interaction and by the differential expression of miRNA. Thus, we propose that these two miRNAs act cooperatively to fine-tune the 'resistance' changes of BmVgR expression for different development stages of different tissues (Fig. 6A,B).

VgRs are highly conserved, not only in their modular structure but also in terms of their regulation among insects (Tufail and Takeda, 2009). Administration of artificial miRNA has been shown to be capable of achieving RNA interference-like effects to cleave selective mRNAs and inhibit the corresponding gene expression (Boden et al., 2004). As bmo-miR-2739 may have a homologue in other insect species and be involved in the regulation of insect egg development by targeting to VgR, it is possible that this small molecule could be used for pest control by feeding or spraying or using transgenic expression in crops to confer protection against insect pests (He et al., 2019). On the other hand, using a miRNA inhibitor to upregulate the expression of VgR and increase the source of nutrients may improve the reproductive capacity in insects of medical and agricultural importance.

Recent studies have documented plenty of discoveries concerning the regulation of certain miRNAs in female insect reproduction. But most of them are limited to Diptera, such as *D. melanogaster*, *A. aegypti*. More research, involving other less-studied insects, is required to reconstruct the evolutionary variation of these miRNAs that govern female insect reproduction. In our study, we discovered

that bmo-miR-2739 and novel-miR-167 are involved in ovarian development by post-transcriptional regulation of *BmVgR* in *B. mori*. bmo-miR-2739 and novel-miR-167 function together to fine-tune the productive translation of the *BmVgR* mRNA to achieve the optimal protein level for ovarian development. novel-miR-167 is mainly responsible for dampening the expression of the weakly expressed *BmVgR* mRNA in non-ovarian tissues. The detailed post-transcriptional repression mechanism of these two miRNAs and the mutually reinforcing mechanism between the two miRNAs in silkworm remain unclear. However, our results suggest that these miRNAs act in a coordinated manner to support stage- and tissue-specific expression of *BmVgR* and contribute to the accumulation of BmVg for oocyte maturation and embryo development. These findings provide fundamental information for the function and evolution of miRNAs in insect reproduction and could be beneficial to the development of pest control approaches and breed improvement.

MATERIALS AND METHODS
Insects and cell lines
The *B. mori* strain Dazao was maintained at Southwest University (Chongqing, China). Fertilized eggs were incubated at 25°C at a humidity level appropriate for hatching. The silkworm larvae were reared on fresh mulberry leaves at 25°C, with a photoperiod of 12 h light/12 h dark and 85% relative humidity.

HEK293T cells were cultured in Dulbecco's modified eagle medium (DMEM) (Gibco), supplemented with 10% (vol/vol) fetal bovine serum (FBS) (Gibco) at 37°C in a 5% CO_2 incubator. A silkworm ovary cell line (BmN4-SID1) was cultured at 27°C in IPL-41 medium (AppliChem) containing 10% (vol/vol) of FBS. *Drosophila* S2 cells were cultured at 27°C in Schneider's *Drosophila* medium (Gibco) containing 10% (vol/vol) FBS.

Small RNA sequencing analysis and *BmVgR* 3′ UTR target microRNA prediction
To prepare the samples for sequencing, ovarioles were dissected at P7D. Total RNA was extracted using TRIzol (Invitrogen), according to the manufacturer's protocol. Construction of a small RNA library was carried out as described in the literature (Huang et al., 2014). Purified PCR

fragments were used for clustering and sequencing by the Illumina Genome Analyzer at the Beijing Genomics Institute, Shenzhen, China. The small RNA libraries have been deposited in the Sequence Read Archive database of National Center for Biotechnology Information (NCBI) (SRA accession: SRP146084).

To identify follicle miRNAs, clean reads were aligned to the mature miRNAs and miRNA precursors of *B. mori* in miRBase 22.0 (http://www.mirbase.org/). We identified novel miRNAs from unannotated clean reads mapped to the silkworm genome by analysing the secondary structure, the Dicer cleavage site, and the minimum free energy (less than or equal to −18 kcal/mol) using miRDeep2, an miRNA prediction program (Friedländer et al., 2008). Then the differential miRNAs were used for target prediction (Table S4).

As we focused on the regulation of BmVgR in follicles, the full-length 3′ UTR of *BmVgR* mRNA was used as a potential target for prediction, using the miRNA target prediction software miRanda (http://www.microrna.org) (Betel et al., 2008). Thresholds were set to a score of 118 and less than −10 kcal/mol in miRanda (Table S5).

Plasmid construction
Full-length *BmVgR* 3′ UTR was amplified from total ovarian cDNA and *BmVgR* 3′ UTR with mutations in bmo-miR-2739 'seed'-binding sites (2739-M1, 2739-M2 and 2739-M3) (Fig. S2A,B). *BmVgR* 3′ UTR with mutations at two binding sites of bmo-miR-2739 (2739-M2+M1), three binding sites of bmo-miR-2739 (2739-M3+M2+M1), and a novel-miR-167 'seed'-binding site (167-M1) (Fig. S2A,B) were synthesized by TSINGKE Biological Technology, Beijing, China. All these fragments were then cloned into a psiCheck-2 vector (Promega) using XhoI and NotI linkers. The resulting reporter plasmids were named psi-*BmVgR* 3′ UTR, psi-2739-M1/2/3, psi-2739-M3+2+1, psi-2739-M2+1 and psi-167-M1. The psiCheck-2 reporter plasmid contained a synthetic *Renilla* luciferase gene (*Rluc*) and synthetic firefly luciferase gene (*luc*) as an internal control. The *Renilla* luciferase signal was normalized to the firefly luciferase signal.

The precursor sequences of bmo-miR-2739 (pre-bmo-miR-2739) and novel-miR-167 (pre-novel-miR-167) were amplified from the silkworm genome. Then the fragments were cloned into a vector (stored in our laboratory) containing the *piggyBac* [3×p3-EGFP, af] basic unit and U6 promoter (Ma et al., 2014) by T4 DNA ligase (New England Biolabs). The polymerase III U6 promoter is capable of synthesizing small nuclear RNA with high yields and is commonly adapted for miRNA synthesis; it also consists of a compact sequence and simple terminator for easy handling (Boden et al., 2004; Zhang et al., 2014; Zhou et al., 2008). The vectors were named *pBac*-U6-2739/n167. All constructs were confirmed by sequencing. The primers used for plasmid construction are listed in Table S1.

Small RNA transfection
miRNA mimics/agomirs and inhibitors/antagomirs were synthesized by RiboBio, Guangzhou, China. The miRNA mimic/agomir was a dsRNA formed with the miRNA and its complementary sequence. The miRNA inhibitors/antagomirs were the antisense oligonucleotide of the miRNA. An miRNA negative control (NC) was designed based on a *Caenorhabditis elegans* miRNA with no similarity to mammalian or insect miRNAs. The sequences are listed in Table S2. All miRNAs were transfected by the ribo*FECT* CP Reagent (RiboBio) in accordance with the manufacturer's protocol.

Dual luciferase reporter (DLR) assay
All reporter plasmids were purified using an EndoFree plasmid kit (Qiagen). For high transfection efficiency and low background expression of targets, the HEK293T cell line and *Drosophila* S2 cells were used for the DLR assay. Cells were seeded in a 48-well plate, then transfected with 300 ng of reporter plasmids using a Lipofectamine 2000 (Invitrogen) reagent, according to the manufacturer's recommendation. Six hours later, synthetic miRNA mimics/agomirs (100-200 nM) and inhibitors (200 nM) were then transfected using the ribo*FECT* CP Reagent. After 24 h, luciferase activity was measured using a Dual Luciferase Reporter Assay Kit (Promega), according to the protocol provided by the manufacturer. Each experiment was performed in triplicate, and the transfections were repeated four times.

RNA isolation and quantitative reverse transcription PCR (qRT-PCR)
Total RNA was extracted using Trizol (Invitrogen), and contaminated genomic DNA was digested by RNase-free DNase I (Takara Bio). Reverse-transcribed miRNAs were synthesized with a Mir-X miRNA First-Strand Synthesis Kit (Takara Bio). For miRNA quantification, the miRNA sequences were used with U converted to T as the forward primers and the mRQ 3′ primer from the Mir-X miRNA First-Strand Synthesis Kit was used as the reverse primers. qRT-PCR analysis was performed using a KAPA SYBR FAST qPCR kit (Kapa Biosystems). The expression levels of the miRNAs were normalized with the small nuclear RNA U6 of *B. mori*.

Reverse transcription to cDNA was performed with the TransScript One-Step gDNA Removal and cDNA Synthesis SuperMix (Transgen Biotech) and carried out according to the manufacturer's instructions. qRT-PCR was performed using SYBR Premix ExTaq (Takara Bio). The silkworm eukaryotic translation initiation factor 4A (*BmTIF4A*) gene was used as an endogenous control.

Both miRNAs and cDNA were detected using an ABI Prism 7500 sequence detection system (Applied Biosystems). Each reaction was performed under the following conditions: denaturation at 95°C for 3 min, followed by 40 cycles of 95°C for 3 s, 60°C for 30 s. The relative mRNA levels of the target genes were calculated using the $2^{-\Delta\Delta C(T)}$ method (Livak and Schmittgen, 2001). The primers for qRT-PCR were designed using Primer Premier 6 software (Table S1).

Western blot
For western blot analysis, proteins were isolated with the lysis buffer RIPA (Beyotime Biotechnology), and concentrations were measured using a BCA assay kit (Beyotime Biotechnology). The proteins were resolved on a 10-15% (w/v) SDS-PAGE gel and then transferred onto a polyvinylidene fluoride (PVDF) membrane (GE Healthcare). The membrane was blocked in 5% (w/v) bovine serum albumin (BSA) in TBST [10 mM Tris-HCl, 150 mM NaCl, and 0.05% (v/v) Tween 20, pH 7.5] at 4°C overnight. Then the membrane was incubated with α-tubulin antibody (1:10,000, T9026, Sigma-Aldrich), β-actin antibody (1:10,000, A1978, Sigma-Aldrich) and anti-BmVg polyclonal rabbit antibody (1:5000; Lin et al., 2013). Anti-BmVgR polyclonal rabbit antibody (recombinant antigen BmVgR amino acid positions 18-216) was expressed with the pCold-SUMO-BmVgR plasmid in *Escherichia coli* strain *Rosetta* (DE3) (TransGen Biotech). Antigen protein, in which the SUMO-tag was cut, was purified using metal-affinity resin (GE Healthcare), then was injected into rabbits for antibody production. Anti-BmVgR polyclonal antibody was purified using antigen-affinity resin at a 1:10,000 dilution for 2 h at room temperature. The membrane was then rigorously washed and incubated with horseradish peroxidase (HRP)-conjugated goat anti-rabbit IgG or goat anti-mouse IgG secondary antibody for 2 h at room temperature. Finally, the signal was visualized using SuperSignal West Femto Maximum Sensitivity Substrate (Thermo Fisher Scientific).

BmVg uptake assays
BmN4-SID1 cells were seeded in two 12-well plates, both of which were transfected with miRNAs-inh (200 nM), 24 h later, incubated with 15 µg/ml purified BmVg for 10 min at 25°C. The cells were lysed using RIPA lysis buffer. This was followed by BmVg protein detection via western blot analysis.

Injection of miRNA antagomir
bmo-miR-2739-antagomir (2739-anta) and novel-miR-167-antagomir (n167-anta) were injected into female silkworms to inhibit the endogenous miRNAs. For each silkworm, 15 µg of miRNA antagomir was injected into the haemolymph at P2D and P4D. A total of 20 animals were injected for each miRNA antagomir. About one-third of the insects were dissected at P8D, and the total RNA was extracted from follicles. The expression levels of the miRNA target genes and VgR protein were then analysed by qRT-PCR and western blot. The remaining pupae were used to observe the phenotype. The experiment was repeated three times.

Generation of transgenic silkworms

The injected embryos were prepared as described in a previous protocol (Tamura et al., 2000). The *piggyBac* transgenic vector *pBac*-U6-2739/n167 together with pHA3PIG vector (stored in our laboratory) were used as the helper plasmid for the production of transposase (Wang et al., 2015) and were microinjected into silkworm embryos 1-2 h after oviposition using a TransferMan NK2 micromanipulator and a Femto Jet 5247 microinjector (Eppendorf) under a SZX16 stereo microscope (Olympus). The injected embryos were incubated at 25°C and 90% relative humidity. The hatched larvae were reared on fresh mulberry leaves and G0 moths were crossed to screen the positive broods in G1 embryos using an Olympus SZX12 fluorescence stereomicroscope.

Inverse polymerase chain reaction (inverse PCR)

Inverse PCR was performed as previously described (Tamura et al., 2000) to locate the insertion sites of integrated *piggyBac* fragments. The genomic DNA was extracted from G1 transgenic moths using a MiniBEST universal Genomic DNA Extraction Kit Ver. 5.0 (Takara Bio). The PCR products were cloned into the pEASY-T5 Zero cloning vector (TransGen Biotech) and their DNA sequences were sequenced and analysed.

Genomic PCR

Genomic DNA was extracted from the larval-to-pupal ecdyses of G1 transgenic silkworms using a 96-format automated DNA isolation system PI-1200 (Kurabo). Genomic PCR was performed with PrimeSTAR Max DNA Polymerase (Takara Bio); the following program was used for PCR: 98°C for 2 min, 30 cycles of 98°C for 10 s, 56°C for 10 s, 72°C for 5 s and 72°C for 2 min. Primer (named 2739-OC and 167-OC) sequences are indicated in Table S1.

Immunofluorescence staining

Ovarioles from female transgenic silkworms and WT silkworms at P6D were fixed overnight at 4°C in 4% (v/v) formaldehyde. Part of a section was treated with the primary antibody, anti-BmVg (1:1000), and then with the secondary antibody, Alexa Fluor 488 goat anti-rabbit IgG (H+L) (1:1000, A11034, Invitrogen), for 1 h to determine the expression pattern of BmVg in the ovary. The cell nuclei were stained with DAPI (Beyotime Biotechnology). The primary and secondary antibodies were diluted 1:500 in PBST [PBS with 0.2% (v/v) Tween 20] and washed with PBST three times after each step. The tissues were fixed onto the glass slide with Antifade Mounting Medium (Beyotime Biotechnology) and examined under a Zeiss LSM 880 confocal microscope.

Statistical analysis

All statistical values are shown as mean±s.e.m. Mean values were compared using unpaired two-tailed Student's *t*-test at the following significance levels: *$P<0.05$ and **$P<0.01$. Statistical analyses were performed using Graph Pad Prism 6.0. Figures were assembled using Adobe Photoshop CS5 and Adobe Illustrator CS5.

Competing interests
The authors declare no competing or financial interests.

Author contributions
Conceptualization: E.C., Q.X.; Methodology: E.C., Z.C., X.J., Y.L., Q.X.; Software: E.C., S. Li, D.X.; Validation: E.C.; Formal analysis: E.C.; Investigation: E.C., H.G., J.L.; Resources: E.C., Z.C., H.G., J.L., X.J., Y.L., Q.X.; Data curation: E.C., Z.C., S. Li, D.X., X.J.; Writing - original draft: E.C., J.L.; Writing - review & editing: E.C., S. Liu, Q.X.; Visualization: E.C., S. Liu, Q.X.; Supervision: S. Liu, Q.X.; Project administration: Q.X.; Funding acquisition: Q.X.

Data availability
The small RNA libraries have been deposited in the Sequence Read Archive database of National Center for Biotechnology Information (NCBI) (SRA accession: SRP146084).

Supplementary information
Supplementary information available online at
http://dev.biologists.org/lookup/doi/10.1242/dev.183723.supplemental

Peer review history
The peer review history is available online at
https://dev.biologists.org/lookup/doi/10.1242/dev.183723.reviewer-comments.pdf

References

Bartel, D. P. (2009). MicroRNAs: target recognition and regulatory functions. *Cell* **136**, 215-233. doi:10.1016/j.cell.2009.01.002

Bartel, D. P. (2018). Metazoan microRNAs. *Cell* **173**, 20-51. doi:10.1016/j.cell.2018.03.006

Bartel, D. P. and Chen, C.-Z. (2004). Micromanagers of gene expression: the potentially widespread influence of metazoan microRNAs. *Nat. Rev. Genet.* **5**, 396-400. doi:10.1038/nrg1328

Bazzini, A. A., Lee, M. T. and Giraldez, A. J. (2012). Ribosome profiling shows that miR-430 reduces translation before causing mRNA decay in Zebrafish. *Science* **336**, 233-237. doi:10.1126/science.1215704

Betel, D., Wilson, M., Gabow, A., Marks, D. S. and Sander, C. (2008). The microRNA.org resource: targets and expression. *Nucleic Acids Res.* **36**, D149-D153. doi:10.1093/nar/gkm995

Boden, D., Pusch, O., Silbermann, R., Lee, F., Tucker, L. and Ramratnam, B. (2004). Enhanced gene silencing of HIV-1 specific siRNA using microRNA designed hairpins. *Nucleic Acids Res.* **32**, 1154-1158. doi:10.1093/nar/gkh278

Bryant, B., Macdonald, W. and Raikhel, A. S. (2010). microRNA miR-275 is indispensable for blood digestion and egg development in the mosquito *Aedes aegypti*. *Proc. Natl. Acad. Sci. USA* **107**, 22391-22398. doi:10.1073/pnas.1016230107

Chen, M. E., Lewis, D. K., Keeley, L. L. and Pietrantonio, P. V. (2004). cDNA cloning and transcriptional regulation of the vitellogenin receptor from the imported fire ant, *Solenopsis invicta* Buren (Hymenoptera: Formicidae). *Insect Mol. Biol.* **13**, 195-204. doi:10.1111/j.0962-1075.2004.00477.x

Chen, Z., Nohata, J., Guo, H., Li, S., Liu, J., Guo, Y., Yamamoto, K., Kadono-Okuda, K., Liu, C., Arunkumar, K. P. et al. (2015). A comprehensive analysis of the chorion locus in silkmoth. *Sci. Rep.* **5**, 16424. doi:10.1038/srep16424

Cho, K. H., Cheon, H. M., Kokoza, V. and Raikhel, A. S. (2006). Regulatory region of the vitellogenin receptor gene sufficient for high-level, germ line cell-specific ovarian expression in transgenic *Aedes aegypti* mosquitoes. *Insect Biochem. Mol. Biol.* **36**, 273-281. doi:10.1016/j.ibmb.2006.01.005

Djuranovic, S., Nahvi, A. and Green, R. (2012). miRNA-mediated gene silencing by translational repression followed by mRNA deadenylation and decay. *Science* **336**, 237-240. doi:10.1126/science.1215691

Dominguez, G. A., Bisesi, J. H., Jr, Kroll, K. J., Denslow, N. D. and Sabo-Attwood, T. (2014). Control of transcriptional repression of the *vitellogenin receptor* gene in largemouth bass (*Micropterus salmoides*) by select estrogen receptors isotypes. *Toxicol. Sci.* **141**, 423-431. doi:10.1093/toxsci/kfu145

Friedländer, M. R., Chen, W., Adamidi, C., Maaskola, J., Einspanier, R., Knespel, S. and Rajewsky, N. (2008). Discovering microRNAs from deep sequencing data using miRDeep. *Nat. Biotechnol.* **26**, 407-415. doi:10.1038/nbt1394

Funaguma, S., Hashimoto, S.-I., Suzuki, Y., Omuro, N., Sugano, S., Mita, K., Katsuma, S. and Shimada, T. (2007). SAGE analysis of early oogenesis in the silkworm, *Bombyx mori*. *Insect Biochem. Mol. Biol.* **37**, 147-154. doi:10.1016/j.ibmb.2006.11.001

Garaulet, D. L., Castellanos, M. C., Bejarano, F., Sanfilippo, P., Tyler, D. M., Allan, D. W., Sánchez-Herrero, E. and Lai, E. C. (2014). Homeotic function of Drosophila Bithorax-complex miRNAs mediates fertility by restricting multiple Hox genes and TALE cofactors in the CNS. *Dev. Cell* **29**, 635-648. doi:10.1016/j.devcel.2014.04.023

Ge, W., Yang, X., Deng, Q., Guo, T., Hong, X., Kugler, J.-M. and Cohen, S. M. (2015). Regulation of pattern formation and gene amplification during *Drosophila* oogenesis by the miR-318 microRNA. *Genetics* **200**, 255-265. doi:10.1534/genetics.115.174748

Goldsmith, M. R., Shimada, T. and Abe, H. (2005). The genetics and genomics of the silkworm, *Bombyx mori*. *Annu. Rev. Entomol.* **50**, 71-100. doi:10.1146/annurev.ento.50.071803.130456

He, J., Chen, Q., Wei, Y., Jiang, F., Yang, M., Hao, S., Guo, X., Chen, D. and Kang, L. (2016). MicroRNA-276 promotes egg-hatching synchrony by up-

regulating *brm* in locusts. *Proc. Natl. Acad. Sci. USA* **113**, 584-489. doi:10.1073/pnas.1521098113

He, K., Xiao, H., Sun, Y., Ding, S., Situ, G. and Li, F. (2019). Transgenic microRNA-14 rice shows high resistance to rice stem borer. *Plant Biotechnol. J.* **17**, 461-471. doi:10.1111/pbi.12990

Huang, Y.-C., Smith, L., Poulton, J. and Deng, W.-M. (2013). The microRNA miR-7 regulates Tramtrack69 in a developmental switch in *Drosophila* follicle cells. *Development* **140**, 897-905. doi:10.1242/dev.080192

Huang, Y., Dou, W., Liu, B., Wei, D., Liao, C. Y., Smagghe, G. and Wang, J.-J. (2014). Deep sequencing of small RNA libraries reveals dynamic expression patterns of microRNAs in multiple developmental stages of *Bactrocera dorsalis*. *Insect Mol. Biol.* **23**, 656-667. doi:10.1111/imb.12111

Izumi, N., Shoji, K., Sakaguchi, Y., Honda, S., Kirino, Y., Suzuki, T., Katsuma, S. and Tomari, Y. (2016). Identification and functional analysis of the pre-piRNA 3′ trimmer in silkworms. *Cell* **164**, 962-973. doi:10.1016/j.cell.2016.01.008

Kawaguchi, Y., Tatsuke, T., Oike, Y., Taniguchi, A., Kusakabe, T., Lee, J. M. and Koga, K. (2008). Fertility and hatching of the *vit* mutant eggs in *Bombyx mori*. *J. Insect Biotechnol. Sericol.* **77**, 121-124.

Kendirgi, F., Swevers, L. and Iatrou, K. (2002). An ovarian follicular epithelium protein of the silkworm (*Bombyx mori*) that associates with the vitelline membrane and contributes to the structural integrity of the follicle. *FEBS Lett.* **524**, 59-68. doi:10.1016/S0014-5793(02)03003-X

Kiuchi, T., Koga, H., Kawamoto, M., Shoji, K., Sakai, H., Arai, Y., Ishihara, G., Kawaoka, S., Sugano, S., Shimada, T. et al. (2014). A single female-specific piRNA is the primary determiner of sex in the silkworm. *Nature* **509**, 633-636. doi:10.1038/nature13315

Lin, Y., Meng, Y., Wang, Y.-X., Luo, J., Katsuma, S., Yang, C.-W., Banno, Y., Kusakabe, T., Shimada, T. and Xia, Q.-Y. (2013). Vitellogenin receptor mutation leads to the oogenesis mutant phenotype "*scanty vitellin*" of the silkworm, *Bombyx mori*. *J. Biol. Chem.* **288**, 13345-13355. doi:10.1074/jbc.M113.462556

Liu, S., Lucas, K. J., Roy, S., Ha, J. and Raikhel, A. S. (2014). Mosquito-specific microRNA-1174 targets serine hydroxymethyltransferase to control key functions in the gut. *Proc. Natl. Acad. Sci. USA* **111**, 14460-14465. doi:10.1073/pnas.1416278111

Livak, K. J. and Schmittgen, T. D. (2001). Analysis of relative gene expression data using real-time quantitative PCR and the $2_T^{-\Delta\Delta C}$ Method. *Methods* **25**, 402-408. doi:10.1006/meth.2001.1262

Lucas, K. J., Roy, S., Ha, J., Gervaise, A. L., Kokoza, V. A. and Raikhel, A. S. (2015a). MicroRNA-8 targets the wingless signaling pathway in the female mosquito fat body to regulate reproductive processes. *Proc. Natl. Acad. Sci. USA* **112**, 1440-1445. doi:10.1073/pnas.1424408112

Lucas, K. J., Zhao, B., Liu, S. and Raikhel, A. S. (2015b). Regulation of physiological processes by microRNAs in insects. *Curr. Opin. Insect Sci.* **11**, 1-7. doi:10.1016/j.cois.2015.06.004

Ma, S., Chang, J., Wang, X., Liu, Y., Zhang, J., Lu, W., Gao, J., Shi, R., Zhao, P. and Xia, Q. (2014). CRISPR/Cas9 mediated multiplex genome editing and heritable mutagenesis of *BmKu70* in *Bombyx mori*. *Sci. Rep.* **4**, 4489. doi:10.1038/srep04489

Nakahara, K., Kim, K., Sciulli, C., Dowd, S. R., Minden, J. S. and Carthew, R. W. (2005). Targets of microRNA regulation in the Drosophila oocyte proteome. *Proc. Natl. Acad. Sci. USA* **102**, 12023-12028. doi:10.1073/pnas.0500053102

Roy, S., Saha, T. T., Zou, Z. and Raikhel, A. S. (2018). Regulatory pathways controlling female insect reproduction. *Annu. Rev. Entomol.* **63**, 489-511. doi:10.1146/annurev-ento-020117-043258

Sappington, T. W. and Raikhel, A. S. (1998). Molecular characteristics of insect vitellogenins and vitellogenin receptors. *Insect Biochem. Mol. Biol.* **28**, 277-300. doi:10.1016/S0965-1748(97)00110-0

Schonbaum, C. P., Perrino, J. J. and Mahowald, A. P. (2000). Regulation of the vitellogenin receptor during *Drosophila melanogaster* oogenesis. *Mol. Biol. Cell* **11**, 511-521. doi:10.1091/mbc.11.2.511

Stark, A., Brennecke, J., Russell, R. B. and Cohen, S. M. (2003). Identification of Drosophila microRNA targets. *PLoS Biol.* **1**, E60. doi:10.1371/journal.pbio.0000060

Swevers, L. and Iatrou, K. (2003). The ecdysone regulatory cascade and ovarian development in lepidopteran insects: insights from the silkmoth paradigm. *Insect Biochem. Mol. Biol.* **33**, 1285-1297. doi:10.1016/j.ibmb.2003.06.012

Tamura, T., Thibert, C., Royer, C., Kanda, T., Abraham, E., Kamba, M., Komoto, N., Thomas, J. L., Mauchamp, B., Chavancy, G. et al. (2000). Germline transformation of the silkworm *Bombyx mori* L. using a *piggyBac* transposon-derived vector. *Nat. Biotechnol.* **18**, 81-84. doi:10.1038/71978

Tanaka, H. (2013). Construction of shRNA expression plasmids for silkworm cell lines using single-stranded DNA and *Bst* DNA polymerase. In *siRNA Design: Methods and Protocols* (ed. D. J. Taxman), pp. 347-355. Totowa, NJ: Humana Press.

Tufail, M. and Takeda, M. (2009). Insect vitellogenin/lipophorin receptors: molecular structures, role in oogenesis, and regulatory mechanisms. *J. Insect Physiol.* **55**, 87-103. doi:10.1016/j.jinsphys.2008.11.007

Wang, F., Wang, R., Wang, Y., Xu, H., Yuan, L., Ding, H., Ma, S., Zhou, Y., Zhao, P. and Xia, Q. (2015). Remobilizing deleted *piggyBac* vector post-integration for transgene stability in silkworm. *Mol. Genet. Genomics* **290**, 1181-1189. doi:10.1007/s00438-014-0982-6

Xia, Q., Zhou, Z., Lu, C., Cheng, D., Dai, F., Li, B., Zhao, P., Zha, X., Cheng, T., Chai, C. et al. (2004). A draft sequence for the genome of the domesticated silkworm (*Bombyx mori*). *Science* **306**, 1937-1940. doi:10.1126/science.1102210

Xia, Q., Guo, Y., Zhang, Z., Li, D., Xuan, Z., Li, Z., Dai, F., Li, Y., Cheng, D., Li, R. et al. (2009). Complete resequencing of 40 genomes reveals domestication events and genes in silkworm (*Bombyx*). *Science* **326**, 433-436. doi:10.1126/science.1176620

Xia, Q., Li, S. and Feng, Q. (2014). Advances in silkworm studies accelerated by the genome sequencing of *Bombyx mori*. *Annu. Rev. Entomol.* **59**, 513-536. doi:10.1146/annurev-ento-011613-161940

Yamauchi, H. and Yoshitake, N. (1984). Developmental stages of ovarian follicles of the silkworm, *Bombyx mori* L. *J. Morphol.* **179**, 21-31. doi:10.1002/jmor.1051790104

Zhang, R. and Su, B. (2009). Small but influential: the role of microRNAs on gene regulatory network and 3′UTR evolution. *J. Genet. Genomics* **36**, 1-6. doi:10.1016/S1673-8527(09)60001-1

Zhang, X., Liu, Q., Luo, C., Deng, Y., Cui, K. and Shi, D. (2014). Identification and characterization of buffalo 7SK and U6 pol III promoters and application for expression of short hairpin RNAs. *Int. J. Mol. Sci.* **15**, 2596-2607. doi:10.3390/ijms15022596

Zhang, Y., Zhao, B., Roy, S., Saha, T. T., Kokoza, V. A., Li, M. and Raikhel, A. S. (2016). microRNA-309 targets the Homeobox gene SIX4 and controls ovarian development in the mosquito *Aedes aegypti*. *Proc. Natl. Acad. Sci. USA* **113**, E4828-E4836. doi:10.1073/pnas.1609792113

Zhang, Q., Sun, W., Sun, B.-Y., Xiao, Y. and Zhang, Z. (2017). The dynamic landscape of gene regulation during *Bombyx mori* oogenesis. *BMC Genomics* **18**, 714. doi:10.1186/s12864-017-4123-6

Zhou, H., Huang, C. and Xia, X. G. (2008). A tightly regulated Pol III promoter for synthesis of miRNA genes in tandem. *Biochim. Biophys. Acta* **1779**, 773-779. doi:10.1016/j.bbagrm.2008.03.011

DEVELOPMENT